Gain Stability Measurements at S-Band and X-Band

S. Gulkis and E. T. Olsen
Atmospheric Sciences Section

The Search for Extraterrestrial Intelligence (SETI) requires low noise broadband total power radiometers of high gain stability. We report here preliminary results of SETI field tests for a variety of receiver configurations at DSS 13. The power spectra of DSN low noise receiving systems exhibit 1/F noise whose spectral index is significantly smaller than unity. The gain stability of the S-band and X-band systems tested is almost 10^{-4}. An appendix presents a derivation of the power spectrum of the output of a square law detector.

I. Introduction

Many physical phenomena exhibit low frequency fluctuations whose power spectral density varies inversely with frequency. These fluctuations are commonly referred to as "1/F noise". In general, the power spectrum of this noise follows the form, F^n, where F is the frequency of the fluctuations and n is the spectral index. The spectral index varies from system to system, but is always near unity. This phenomenon has been observed in the current output from junction diodes, zener diodes, and schottky diodes, in the frequency of quartz oscillators, and in the voltage gain of amplifiers.

In a total power radio astronomy receiving system, the detected power exhibits 1/F noise in combination with thermal ("white") noise which has a spectral index of zero. The frequency dependent noise is generally attributed to gain variations in the amplifiers arising from a number of physical sources, such as variations in the power supplies, temperature, pump power levels, and mechanical vibrations. The contribution of the atmosphere to the fluctuations in system temperature is also important at X-band and higher frequencies. Under certain circumstances, the 1/F noise in these systems will dominate the thermal noise, and the system sensitivity can be severely degraded from what is predicted based on the system temperature.

The rms temperature fluctuations of the output of a total power receiver is given approximately by the expression (Ref. 1):

$$\Delta T = T\left[(B\tau)^{-1} + (\Delta G/G)^2\right]^{1/2} \qquad (1)$$

where T is the system temperature, G is the average predetection power gain, ΔG is an effective value of the power gain variation, B is the predetection bandwidth and τ is the integration time. The first term of the expression in the square brackets is due to the thermal noise (Johnson noise). The second term is due to the gain fluctuations. It is clearly seen from equation (1) that the gain fluctuations assume greater significance as $B\tau$ is increased. A more complete discussion of Equation (1) is given in Appendix A.

The frequency at which the 1/F noise becomes equal to the white noise is sometimes referred to as the "knee fre-

quency". This "knee frequency" is a function of the predetection bandwidth, and hence needs to be specified in order to provide a complete description. At frequencies lower than the knee frequency, the 1/F noise dominates the system fluctuations; at frequencies higher than the knee frequency, the thermal noise dominates. It is important to know where the transition occurs in order to be able to estimate the sensitivity of a receiving system.

The SETI program intends to utilize the NASA Deep Space Network receiving systems over a wide range of bandwidths, integration times, and microwave frequencies. As a first step toward understanding the nature of the noise in DSN receiving systems, we measured the power spectra of S-band and X-band receiving systems situated at DSS 13, the 26m R&D (Venus) station located at Goldstone, California. From these measurements, we were able to obtain both the spectral index of the 1/F noise and the knee frequency. The results of these measurements are reported here.

II. Experiment Configuration

We tested the three different system configurations shown in Fig. 1. Configuration A is known as the S-band VLBI receiver configuration. The instantaneous bandpass of this receiver was measured to be 14 MHz between the 3 dB points. Configuration B is the S-band R&D receiver in combination with the microwave link from DSS 13 to DSS 14. The instantaneous bandpass of this receiver configuration was set by the 5 MHz bandpass of the microwave link. Configuration C is the X-band VLBI receiver. The instantaneous bandpass of this receiver was measured to be 25 MHz between the 3 dB points. The system noise temperatures of these systems are approximately 30 K at S-band and 33 K at X-band.

Figure 2 shows a block diagram of the instrumentation used to measure the gain stability. The receiver intermediate frequency (IF) is input to a broadband (1 MHz to 130 MHz) square law detector. The detector DC output is then converted to frequency in the analog to digital (A/D) converter by a fast VCO (Analog Devices 460L V/F converter). This frequency is then counted and sampled by an HP 9825A desk top computer at a 210 Hz rate. The accumulation times are selectable and the power spectra are computed as described in the following section.

III. Experimental Procedure

The complete system was turned on and allowed time to stabilize; subsequently the system noise temperature was calculated by switching the receiver input from the sky to an ambient load of known temperatures. The A/D converter linearity and offset had already been measured prior to its arrival at Goldstone. With the IF from the receiving system connected, the power level output from the detector was adjusted so that the digital voltmeter which monitored the system displayed a reading of 0.5 volts. This value was chosen because it is in the middle of the dynamic range of the A/D converter. The output of the converter was then sampled and analyzed using the HP 9825A. The time constant for the sampling, the number of points in the fast fourier transform (FFT), and the number of integrations to be added together were specified in response to prompts from the HP 9825A. Following the completion of a data sampling run, the power spectrum is computed and the result displayed on the HP plotter. In order to obtain a wide range of frequencies in the power spectrum, we combined the results of several data runs with different integration times. The power spectral density was computed for each run and the results of several runs were combined in a single plot. The FFT algorithm utilized is based on one given for real functions by Brigham (Ref. 2). The input to the FFT is 2^N $(1 < N < 10)$ points, and the power spectrum output is:

$$P(n/T) = (a_n^2 + b_n^2)/2 \qquad (2)$$

where $n = 1, 2, 3, \ldots, 2^{N-1}$ and the input time series may be written as a Fourier series:

$$D(t) = a_o/2 + \sum_n [a_n \cos(2\pi nt/T) + b_n \sin(2\pi nt/T)] \qquad (3)$$

over the interval $0 < t < T$.

Each point in the power spectrum is normalized by the total power contained within the spectrum. Thus the output is a normalized power. An average power spectrum is produced by accumulating the power spectra from many individual runs.

IV. Experimental Results

Figure 3 shows the power spectrum of the S-band VLBI receiver (configuration A). The frequency range spanned by the data is 0.1 Hz to 10 Hz. The data represented by open circles were acquired while the receiver system was looking out the horn; the data represented by filled circles were acquired while the receiver system was connected to an ambient temperature load. The power spectrum increases rapidly for temporal frequencies below 1 Hz, and we identify this rapid increase with the 1/F noise component. The spectral index of the 1/F noise component is $n = -0.83$, and the knee frequency is 1.3 Hz. Since the open and filled circles are

nearly coincident, we conclude that the measured 1/F noise spectrum is dominated by the receiving system itself and not by the atmosphere. We note that there is a slight increase in the noise power of the system when it is viewing the sky; this may be due to the atmosphere being less stable than the ambient load.

Figure 4 shows the power spectrum of the S-band VLBI receiver over a much wider range (2×10^{-4} Hz to 50 Hz) than is shown in Fig. 3. While the signal-to-noise ratio of this spectrum is poor due to the small number of individual power spectra which were combined, it nevertheless shows that the 1/F noise component extends to 2×10^{-4} Hz with little change in slope.

Figures 5 and 6 show power spectra for the X-band VLBI receiver (configuration C). These figures correspond to Figs. 3 and 4 respectively. The 1/F noise component spectral index is $n = -0.78$, and the knee frequency is 1.5 Hz.

Thus there is no significant difference apparent in the gain stability of the two VLBI receiving systems at DSS 13. Both exhibit a spectral index of approximately −0.8 and a knee frequency of 1.4 Hz.

Figure 7 shows the power spectrum for the S-band R&D receiver (configuration B) as seen at the end of the microwave link at DSS 14. The 1/F noise component spectral index is $n = -0.8$ and the knee frequency is 1.2 Hz. Aside from the fact that the bandwidth of the link is 5 MHz (which should make the thermal noise component larger, shifting the knee frequency to a slightly lower frequency), we can see that no additional fluctuations were imposed by the link. The spectral index of this system is within the experimental uncertainty of the measurements of the values for configurations A and C.

V. Conclusions

The gain of the S-band and X-band receiving systems is stable to approximately three parts in 10^4. The spectral index of the 1/F noise for the three configurations tested is 0.8 ±0.03, significantly smaller than unity. This exceeds the requirements of the 1 kHz resolution leg of the SETI target survey for an accumulation time of 1000 seconds. It is very close to meeting the radio astronomy requirements of the SETI all sky survey. The high gain stability is required for a continuum survey which utilizes the full 256 MHz bandpass and may accumulate for as long as 3 seconds.

The authors suggest that a standardized procedure be implemented on a trial basis to determine if monitoring the gain stability might provide an early warning that a receiving system is beginning to deteriorate.

VI. Future Work

The tests reported here were by no means exhaustive. Listed below are some of the areas where future studies would be useful.

(1) The knee frequency for a system is expected to vary with the bandwidth of the system. We did not explore this variation in our experiments. Some tests should be carried out using varying bandpasses.

(2) Some small broad features were apparent in power spectra accumulated overnight. Investigations with increased signal-to-noise should be made to determine if these features are indeed present and to understand them if they are.

(3) Increase the sampling rate beyond the 50 Hz limit imposed by our equipment. We just missed the expected 60 Hz feature, and it would be useful to trace this out, as well as to look for its higher harmonics.

(4) Extend the measurements to even lower frequencies to see if there is a break in the 1/F spectrum. This would mean that another component, with 1/F noise of a different slope, has become predominant.

(5) Repeat the tests for the R&D receiver and VLBI receiver with the detection setup on each side of the microwave link.

(6) Extend the tests to DSS 14 receivers, and in particular make measurements of the K-band system.

(7) Repeat the tests over different times to sort out diurnal effects and the effects of the atmosphere.

(8) Extend the work to include cooled and room temperature FET systems, as these systems are likely to show a spectral index different than those of the maser systems.

Note

After this paper was written, the authors became aware of another treatment of this topic for the case of a 94-GHz receiver in a laboratory environment (see Ref. 4).

References

1. Kraus, J. D., *Radio Astronomy*, McGraw-Hill, 1966, pp 247-248.
2. Brigham, E. O., *The Fast Fourier Transform*, Prentice-Hall, New Jersey, 1974.
3. Campbell, "Mathematical Analysis of Random Noise," in *Noise and Stochastic Processes*, N. Wax, ed., Dover Publications, 1954, p. 281.
4. Hersman, Michael S., and Poe, Gene A., "Sensitivity of the Total Power Radiometer with Periodic Absolute Calibration," in *IEEE Transactions on Microwave Theory and Techniques*, Vol MITT-29, pp. 32-40, Jan. 1981.

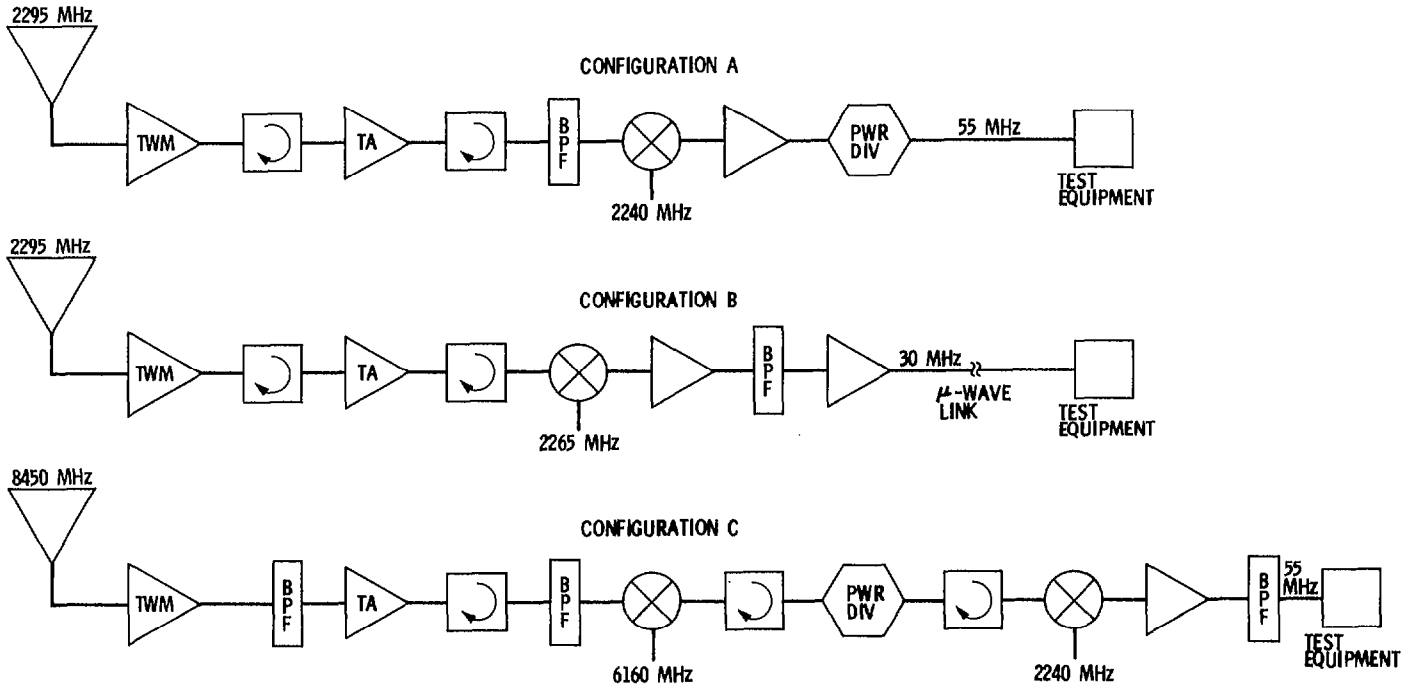

Fig. 1. The three receiver configurations tested: Configuration A is the DSS 13 S-band VLBI receiver; Configuration B is the DSS 13 S-band R&D receiver in combination with the microwave link from DSS 13 to DSS 14; Configuration C is the DSS 13 X-band VLBI receiver

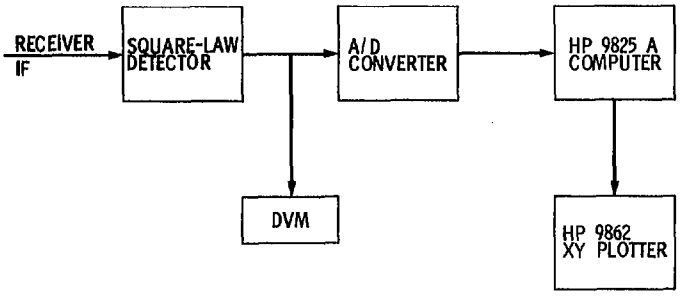

Fig. 2. The block diagram of the instrumentation used to measure the gain stability

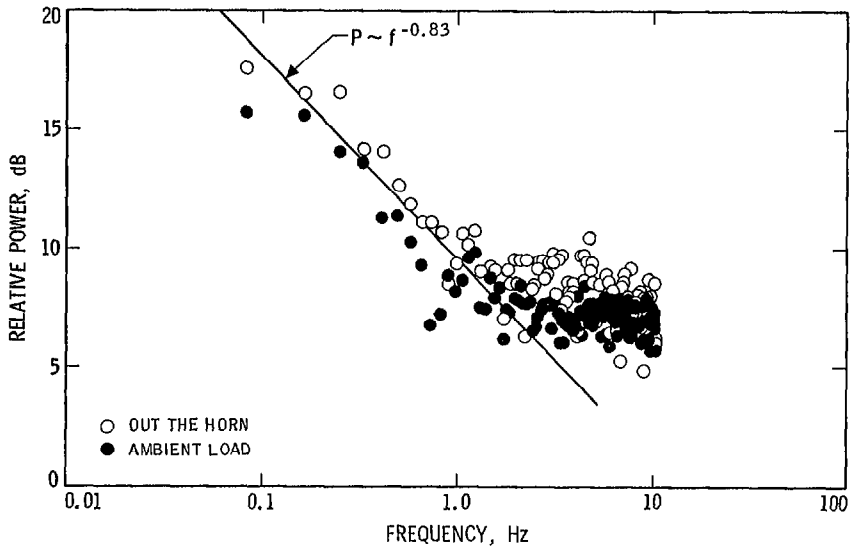

Fig. 3. The power spectrum of the gain fluctuations of the S-band VLBI receiver (Configuration A) over the frequency range 0.1 to 10 Hz. Open circles represent data taken looking out the horn with the antenna pointed at the zenith. Filled circles represent data taken looking at an ambient load

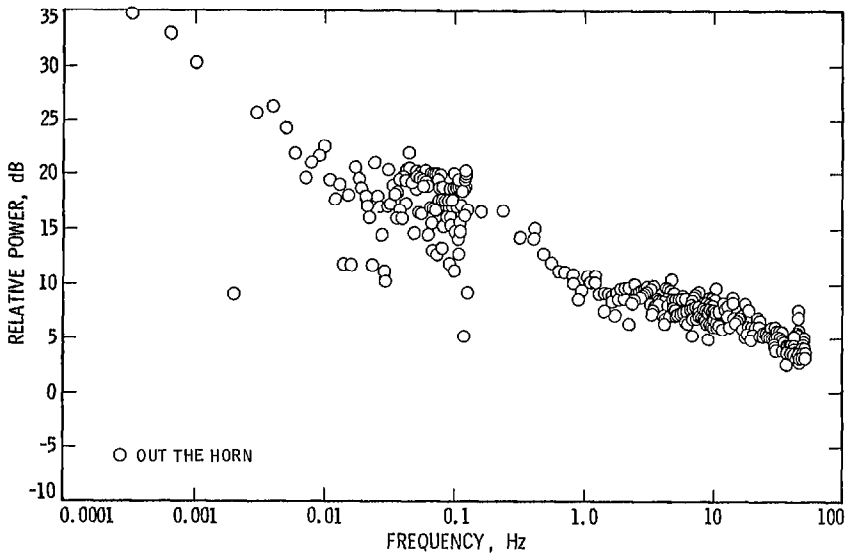

Fig. 4. The power spectrum of the gain fluctuations of the S-band VLBI receiver (Configuration A) over the frequency range 10^{-4} to 50 Hz. The receiver was looking out the horn while the antenna was pointed at the zenith

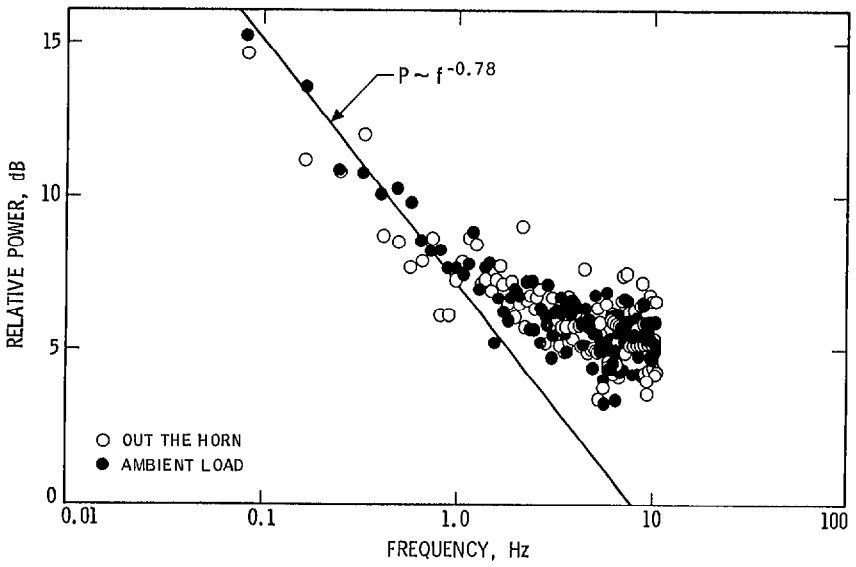

Fig. 5. The power spectrum of the gain fluctuations of the X-band VLBI receiver (Configuration C) over the frequency range 0.1 to 10 Hz. Open circles represent data taken looking out the horn with the antenna pointed at the zenith. Filled circles represent data taken looking at an ambient load

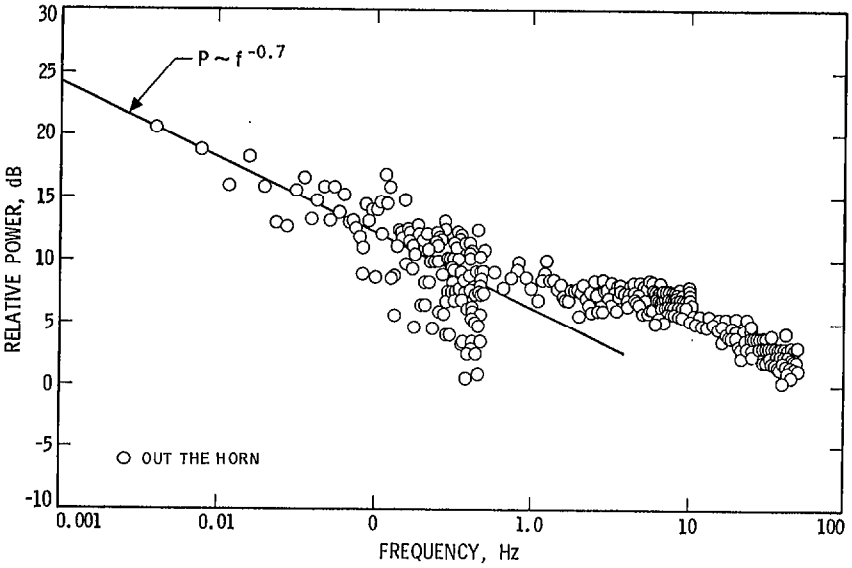

Fig. 6. The power spectrum of the gain fluctuations of the X-band VLBI receiver (Configuration C) over the frequency range 10^{-4} to 50 Hz. The receiver was looking out the horn while the antenna was pointed at the zenith

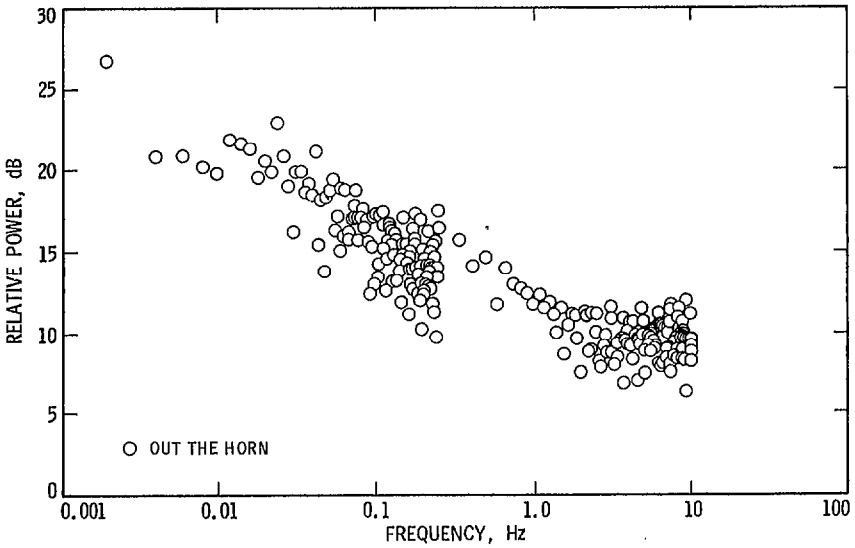

Fig. 7. The power spectrum of the gain fluctuations of the S-band R&D receiver as seen at the end of the microwave link at DSS 14. The receiver was looking out the horn while the antenna was pointed at the zenith

Appendix

The Power Spectrum of a Square Law Detector with Gain Variations

We present in this appendix a derivation of the power spectrum of the output of a square law detector which exhibits its gain fluctuations. Let us first consider the power spectrum of the output of a square law detector whose gain, G, is constant. Assume that the output from the detector is given by:

$$D(t) = G\,V^2\,(t) \tag{A-1}$$

where $V(t)$ is the input voltage as a function of time. The correlation function of $D(t)$ when $V(t)$ is the result of thermal noise only is given by:

$$\psi(\tau) = G^2\,[\psi_0^2 + 2\,\psi_\tau^2] \tag{A-2}$$

where ψ_τ is the correlation function of the noise voltage, $V(t)$ (Ref. 3).

In the frequency domain, the power spectrum of the detector output is given by:

$$\phi(f) = G^2\,[\psi_0^2\,\delta\,(f) + 2\int_{-\infty}^{\infty} w(f)\,w(f-z)\,dz] \tag{A-3}$$

where

$$w(z) = \int_{-\infty}^{\infty} \psi_\tau\,e^{-i2\pi z\tau}\,d\tau \tag{A-4}$$

is the power spectral density of $V(t)$ and $\delta(f)$ is the unit impulse at $f = 0$. Fig. A-1 shows the power spectral density of bandlimited thermal noise; Fig. A-2 shows the power spectrum which corresponds to the bandlimited thermal noise spectrum shown in Fig. A-1.

Let us assume that the gain is a fluctuating quantity, but that $\Delta G/G \ll 1$, so that it may be written:

$$G(t) \cong G_0 + \Delta G(t) = G_0\,[1 + \Delta G(t)/G_0] \tag{A-5}$$

Substituting this approximation for $G(t)$, we may rewrite Eq. (A-1) in the following form:

$$D(t) = G_0\,[1 + \Delta G/G_0]\,V^2\,(t) \tag{A-6}$$

and the correlation function for $D(t)$ is:

$$\psi_G(\tau) = G_0^2\,\psi(\tau)\,\overline{[(1 + \Delta G(t)/G_0)\,(1 + \Delta G(t+\tau)/G_0)]} \tag{A-7}$$

where the term in brackets is the autocorrelation function of the normalized gain.

Since the power spectrum is the Fourier transform of the correlation function, the product relationship in Eq. (A-7) implies that the power spectrum of $D(t)$ is derived by convolving the power spectrum given by Eq. A-3 with the power spectrum of the gain fluctuations. This convolution leads to the following approximate expression for the power spectrum of the output of a square law detector which suffers gain fluctuations:

$$\phi_G(f) = (kTB)^2\,\delta(f) + (kT)^2\,(B - f) + (kTB)^2\,g(f) \tag{A-8}$$

where $g(f)$ is the power spectrum of the gain fluctuations. The convolution of $g(f)$ with the distributed part of $\phi(f)$ has been dropped in this expression because it is generally small.

The part of Eq. (A-8) which contains a delta function in frequency, $\delta(f)$, represents the DC power in the spectrum. The variance around the mean of $D(t)$ is:

$$\Delta P^2 = \int_0^{\infty} [(kT)^2\,(B - f) + (kTB)^2\,g(f)]\,df \tag{A-9}$$

Equation (A-9) leads directly to Eq. (1) if we realize that the total system power is $P = kTB$ and the frequency interval is the reciprocal of the integration time, τ. Thus we may rewrite Eq. (A-9):

$$\Delta P^2/P^2 = (B\tau)^{-1} + \int_0^{f_{max}} g(f)\,df \tag{A-10}$$

and since we recognize:

$$\int_0^{\infty} g(f)\,df = \psi_G(0) = \overline{(\Delta G/G)^2} \tag{A-11}$$

we see that Eq. (A-10) is just another way of writing Eq. (1):

$$\Delta P^2/P^2 = (B\tau)^{-1} + \overline{(\Delta G/G)^2} \tag{A-12}$$

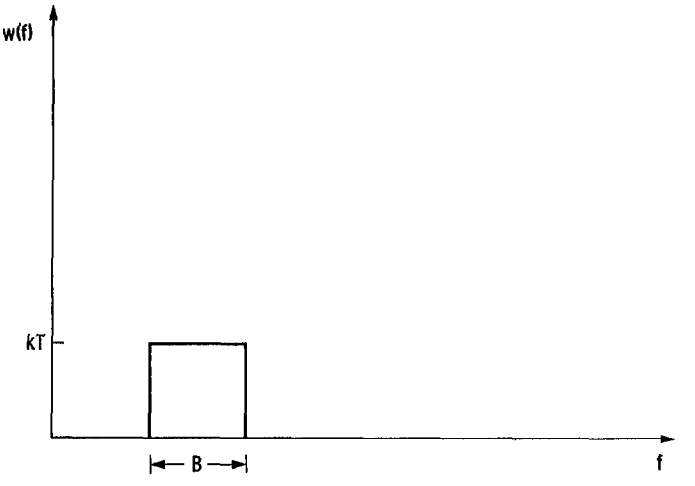

Fig. A-1. The power spectral density of bandlimited thermal noise

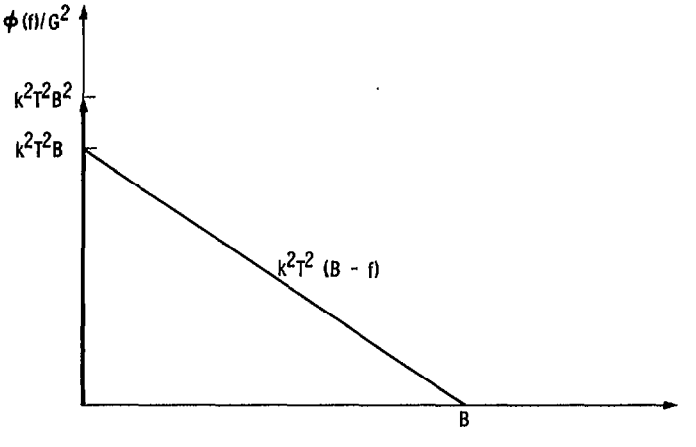

Fig. A-2. The power spectrum of the bandlimited thermal noise spectrum shown in Fig. A-1